Supplementary Information

Copper-hollow mesoporous polydopamine-polyacrylic acid nanoplatform enabling photoacoustic imaging-guided photothermal/chemodynamic therapy for osteosarcoma

Haoyu Sun[1], Zeping Liu[1], Bowen Chen[2], Yunkai Bao[3,4], Fenghua Li[3,4], Rui Gu[1*], Zhenxin Wang[3,4]

[1]Department of Orthopaedic Surgery, China-Japan Union Hospital of Jilin University, Changchun, 130033, PR China.

[2]Department of Thyroid Surgery, General Surgery Center, The First Hospital of Jilin University, Changchun 130021, Jilin, China.

[3]Key Laboratory of Electroanalytical Chemistry, Changchun Institute of Applied Chemistry, Chinese Academy of Sciences, Changchun 130022, Jilin, China.

[4]University of Science and Technology of China, Hefei 230026, Anhui, China.

*Corresponding author:

E-mail address: *gurui@jlu.edu.cn*

Contents

1 Additional Experimental Section

2 Additional Figures S1-S13

3 Additional Tables S1-S2

4 Additional References

1 Additional Experimental Section

Materials

Dopamine Hydrochloride (99%), 1, 3, 5-trimethylbenzene (TMB), pluronic F127 (F127) , $CuCl_2 \cdot 2H_2O$ and sodium polyacrylate (PAA, Mw = 4500 g mol^{-1}, PDI ⩽1.5) were purchased from Aladdin Reagent Co., Ltd. (Shanghai, China). Calcium green acetoxymethyl ester (Calcium Green AM) and propidium iodide (PI) were purchased from Beyotime Biotechnology Co., Ltd. (Jiangsu, China). 3-(4,5-Dimethylthiazol-2-yl)-2,5-diphenyltetrazolium bromide (MTT) was purchased from Jiangsu Keyuan Biotechnology Co., Ltd. Dulbecco's Modified Eagle's Medium (DMEM) and fetal bovine serum (FBS) were purchased from Gibco (New York, USA). The trypsin cell dissociation kit was purchased from Beijing Solarbio Science & Technology Co., Ltd. (Beijing, China). Other reagents were obtained from Beijing Chemical Reagent Co., Ltd. (Beijing, China). All chemicals were of analytical grade and used as received without further purification. Milli-Q water (18.2 MΩ cm) was used in all experiments.

Characterization

The morphology of the nanoparticles (NPs) was recorded using a Hitachi H-600 electron microscope (Hitachi Ltd., Japan) at an accelerating voltage of 100 kV. X-ray photoelectron spectroscopy (XPS) measurements were carried out using a VG ESCALAB MKII spectrometer (VG Scientific Ltd.,UK). Zeta potential and hydrodynamic size measurements were conducted on a Malvern Zetasizer (Malvern Instruments Ltd., UK). The MTT assay was performed using a Versamax microplate reader (Bio-Tek Instruments, Inc., USA). UV-Visible spectra were recorded using a Mini 1240 UV-Visible spectrophotometer (Shimadzu Co., Japan). The PA imaging was conducted on a multispectral optoacoustic tomography imaging system (MSOT in Vision 128, iThera Medical GmbH, Germany). Fluorescence images were obtained using a confocal laser scanning microscope (CLSM, Nikon Co., Japan). Infrared (IR) thermal images were captured on a Ti400 thermal imager (Fluke Co., USA) and analyzed with Smart View software.

Synthesis of HMPDA NPs

The HMPDA NPs were prepared by a previously reported method with slight modification.[1, 2] A typical procedure was as follows. Pluronic F127 (0.4 g) and 1,3,5-trimethylbenzene (TMB, 0.4 g) were dissolved in a mixed solvent consisting of deionized water (70 mL) and ethanol (65 mL), followed by stirring for 30 min. Subsequently, a Tris solution (100 mg dissolved in 10 mL deionized water) was added to the mixture, followed by the addition of dopamine hydrochloride (60 mg). The resulting solution was incubated in a water bath at 28 °C under dark conditions with continuous stirring for 24 h. The resulting NPs were collected by centrifugation at 10,000 rpm for 10 min and washed three times with a mixture of ethanol and acetone (2:1, v/v) using ultrasonication for 30 min each time. Finally, the purified HMPDA NPs were redispersed in ethanol for further use.

Synthesis of HMPDA-Cu NPs

Tris buffer solution (10 mM, pH 8.5) and ethanol were mixed at a volume ratio of 2:1. Subsequently, 0.5 mL of HMPDA ethanol solution (0.6 mg mL^{-1}) and 10 mL of $CuCl_2$ (25 mg mL^{-1}) were added sequentially. The mixture was stirred continuously at 28 °C in the dark for 2 h. Afterward, the HMPDA-Cu NPs were collected by centrifugation at 10,000 rpm for 10 min, washed three times with deionized water (10 mL each), and finally redispersed in 10 mL of deionized water.

Synthesis of HMPDA-Cu@PAA NPs

10 mL PAA solution (3% wt/v) were added into 100 mL of HMPDA-Cu nanoparticle suspension (300 μg mL^{-1}). The mixture was continuously stirred at 28 °C for 2 h. Afterward, the HMPDA-Cu@PAA NPs were collected by centrifugation at 10,000 rpm for 10 min, washed three times with deionized water (10 mL each), and finally redispersed in 10 mL of deionized water.

In Vitro Depletion of GSH by HMPDA-Cu@PAA NPs

50 μL HMPDA-Cu@PAA NPs at different concentrations (800, 400, 200, 100, and 50 μg mL^{-1}) were mixed with 950 μL of GSH solution (20 μmol L^{-1} in PBS, pH 7.4). After incubating the mixture at 37 °C for 1 h, the mixture was centrifuged at 10000 rpm for 10 min. The supernatant was collected, and the residual GSH

concentration was quantified using a commercial GSH assay kit according to the manufacturer's protocol.

Detection of Extracellular ·OH

The MB could be degraded by ·OH, different concentrations of HMPDA-Cu@PAA NPs were added to 2 mL of MB oxygen-free solution (8 mg L^{-1}) at pH 7.4 (in dibasic sodium phosphate-citric acid buffer solution) to establish an adsorption/desorption. After stirring for different times, different concentrations of H_2O_2 were added to the mixture, and the degradation of MB was assessed by UV-Vis absorption spectroscopy to evaluate the effects of reactant concentration, reaction time, and H_2O_2 concentration on·OH formation. Similarly, the effects of temperature and pH on ·OH formation were assessed by increasing the temperature and setting different pH values.

The ·OH production levels of HMPDA-Cu@PAA NPs were determined by TMB and electron paramagnetic resonance (EPR) spin-trapping experiments. HMPDA-Cu@PAA (100 μg mL^{-1}) was dispersed in PBS (pH 6.5) and incubated with H_2O_2 (100 μM) and TMB (60 μg mL^{-1}) at a predetermined time. The suspension was collected by centrifugation to determine the ·OH production by UV-Visible spectra. To measure ·OH generation by EPR, the HMPDA-Cu@PAA NPs was reacted with H_2O_2 (100 μM) for 30 min and mixed with 5,5-dimethyl-1-pyrroline N-oxide (DMPO) aqueous solution for measurement.

The photothermal effect of HMPDA-Cu@PAA NPs

100 μL HMPDA-Cu@PAA at different concentrations (0.05, 0.1, and 0.2 mg mL^{-1}) were irradiated with an 808 nm NIR laser at different power densities (0.5, 1.0, and 2.0 W cm^{-2}) for 600 s. For the heating and cooling experiments, 100 μL HMPDA-Cu@PAA NPs (0.1 mg mL^{-1}) were irradiated with an 808 nm NIR laser at a power density of 2.0 W cm^{-2} for 600 s, after which the laser was turned off, and the solution was allowed to cool naturally.

Cell culture

The MG63 cell line was purchased from Shanghai Fuheng Biotechnology Co., Ltd. (Shanghai, China), which is affiliated with the Chinese Academy of Sciences

(CAS). The MG63 cells were cultured in DMEM medium containing 10% FBS and 1% streptomycin-penicillin, which were placed into cell culture incubator at 37 ℃ and 5% CO_2.

The MTT assay

The MTT assay was used to evaluate cell proliferation. MG63 cells were seeded into 96-well plates at a density of 1×10^4 cells per well and incubated overnight with one of the following treatments: PBS, 100 μM H_2O_2, HMPDA-Cu@PAA NPs, HMPDA-Cu@PAA NPs plus 100 μM H_2O_2, HMPDA-Cu@PAA NPs plus 808 nm NIR laser, or HMPDA-Cu@PAA NPs plus 808 nm NIR laser and 100 μM H_2O_2. For the NIR-irradiated groups, the plates were exposed to an 808 nm laser at a power density of 2.0 W cm^{-2} for 10 min. After a further 18 h incubation, 10 μL of MTT solution was added to each well and incubated for 4 h at 37 °C. The optical density (OD) at 570 nm was measured using a microplate reader, and relative cell viability was calculated as (OD_{570} sample / OD_{570} control) × 100%.

Calcein-AM and PI staining

MG63 cells were co-incubated with PBS, 100 μM H_2O_2, HMPDA-Cu@PAA NPs, HMPDA-Cu@PAA NPs plus 100 μM H_2O_2, HMPDA-Cu@PAA NPs plus 808 nm near-infrared (NIR) laser, or HMPDA-Cu@PAA NPs plus 808 nm NIR laser and 100 μM H_2O_2. For the NIR laser irradiation group, after 6 h of co-incubation, the cells were irradiated with NIR laser (808 nm, 2 W cm^{-2}, 10 min). After 18 h, MG63 cells were stained with AM (10 ng mL^{-1}, 1 mL) and PI (10 ng mL^{-1}, 1 mL) and observed under a fluorescence microscope.

Wound healing assay

MG63 cells were seeded in 6-well plates at 2×10^5 cells per well and cultured overnight to approximately 80% confluence. Then a uniform linear scratch was created using a 100 μL pipette tip. After the different treatments, cells in the NIR groups were co-incubated for 6 h and then irradiated with an 808 nm laser at a power density of 2.0 W cm^{-2} for 10 min. Following a further 18 h of incubation, and the cells

were washed three times with PBS. Images were acquired at 0 and 48 h using a light microscope.

Transwell cell invasion assay

MG63 cells treated with different groups were seeded into Transwells (3×10^4 cells per well) for the invasion assay, using Matrigel to assess the cells' invasive capacity. After 24 h of incubation, non-invading cells were removed. The invasive cells were fixed with 4% paraformaldehyde, stained with crystal violet, and then observed and photographed under an inverted biological microscope.

Detection of Intracellular ROS Production.

MG63 cells were seeded into a 96-well plate and incubated for 24 h. Then, the cells were cultured with DCFH-DA (1 μmol L^{-1} in DMEM) for 20 min. Afterward, the medium was replaced with acidified medium (pH 6.5) containing100 μM H_2O_2, normal medium containing 100 μg mL^{-1} HMPDA-Cu@PAA, and acidified medium (pH 6.5) containing 100 μg mL^{-1} HMPDA-Cu@PAA NPs and 100 μM H_2O_2. The cells were cultured in normal medium containing 100 μg mL^{-1} HMPDA-Cu@PAA NPs and in acidified medium (pH 6.5) containing 100 μg mL^{-1} HMPDA-Cu@PAA NPs and 100 μM H_2O_2, and then they were irradiated with 808 nm NIR laser for 10 min. The cells were cultured by the normal culture as the control sample. After 2 h, the cells were washed with PBS (100 μL, three times). Intracellular ROS was evaluated by detecting the fluorescence of DCF (λex = 488 nm, λem = 525 nm) using a confocal laser scanning microscope.

Animal models

BALB/c nude mice (6-8 weeks old, 20 g average body weight), were purchased from Vita River Laboratory Animal Technology Co., Ltd. (Beijing, China). The Animal Welfare and Research Ethics Committee of Jilin University approved all experimental animal procedures (Approval number: SY 202512006). The laboratory mice were housed under controlled conditions, namely 20-23 ℃ (± 0.5 ℃), 50-70% (± 10%) relative humidity, and a 12 h : 12 h light: dark cycle. Water and food were available ad libitum for all animals.

Photoacoustic (PA) imaging of HMPDA-Cu@PAA NPs

The PA imaging was conducted on a multispectral optoacoustic tomography imaging system. *In vivo*, PA imaging capacity was evaluated after i.v. of HMPDA-Cu@PAA NPs (The dosage of HMPDA-Cu@PAA NPs was 15 mg kg^{-1}) in the mouse-bearing osteosarcoma tumor model. The PA images of the tumor at a different time (0, 6, 12, and 24 h) were obtained.

***In vivo* Photothermal Imaging**

Tumor-bearing mice were intravenously injected with 0.1 mL of PBS, HMPDA-Cu@PAA NPs (15 mg kg^{-1}). After injection, in vivo thermal imaging was conducted using an infrared camera. At 12 h post-injection, the tumor tissues were exposed to an 808 nm laser (2 W cm^{-2}) for 10 min, and thermal photographs along with corresponding temperature values were captured.

***In vivo* synergistic therapy**

Female BALB/c nude mice (6-8 weeks old, 20 g average body weight) were used to establish the osteosarcoma tumor model. MG63 cells (1×10^6 in 100 μL of PBS) were subcutaneously injected into the right dorsal region of the mice. When the tumors grew to 4-5 mm in diameter, the mice were randomly divided into four groups (n=3) and treated as follows: (1) PBS, (2) PBS plus 808 nm NIR laser, (3) HMPDA-Cu@PAA NPs (15 mg mL^{-1} in PBS), and (4) HMPDA-Cu@PAA NPs, (15 mg kg^{-1}) plus 808 nm NIR laser. For PTT, the tumors were irradiated with 808 nm NIR laser (2 W cm^{-2}) for 10 min at 12 h post-injection. Tumor volume was calculated using the formula:

$$\text{Volume (tumor)} = (\text{tumor length} \times \text{tumor width}^2) / 2$$

The tumor inhibition rate (TIR) was calculated as follows:

$$TIR = (1 - V_E/V_C) \times 100\%$$

Where V_E is the average tumor volume of experimental group, V_C is the average tumor volume of control group.

Biocompatibility Experiment

Red blood cell suspension (4% volume fraction) was supplemented with

HMPDA-Cu@PAA to prepare suspensions ranging from 100 μg mL^{-1} to 1000 μg mL^{-1}. Following a 4-hour incubation at 25 °C, the supernatant's absorbance was measured at 577 nm for calculating hemolysis percentage.

***In vivo* Toxicology Analysis**

HMPDA-Cu@PAA NPs (15 mg mL^{-1} in PBS) were injected intravenously into the mice. After 14 days of injection, heart, liver, spleen, lung, kidneys, muscle, and tumor were sliced and stained with hematoxylin and eosin (H&E) staining and TUNEL staining. For blood analysis, healthy BALB/c nude mice were injected intravenously with HMPDA-Cu@PAA NPs, and PBS. Afterward, comprehensive blood routine tests and liver function assessments were carried out.

For biodistribution analysis

For biodistribution analysis. the MG63 tumor-bearing BALB/c nude mice were sacrificed at 6,12 and 24 h post injection of the HMPDA-Cu@PAA NPs. The tissues (tumor, heart, liver, spleen, lung and kidneys) were collected and digested in aqua regia at 80 ℃ for 6 h. The amounts of Cu element in the as-obtained liquids were detemined by Inductively Coupled Plasma Mass Spectrometer (ICP-MS).

Statistical Analysis

Data are expressed as mean ± standard deviation (SD). Statistical significance was determined using the Student's t-test with SPSS statistics 22. In this study, statistical significance was defined as $*P < 0.05$, $**P < 0.01$, and $***P < 0.001$.

2 Additional Figures S1-S13

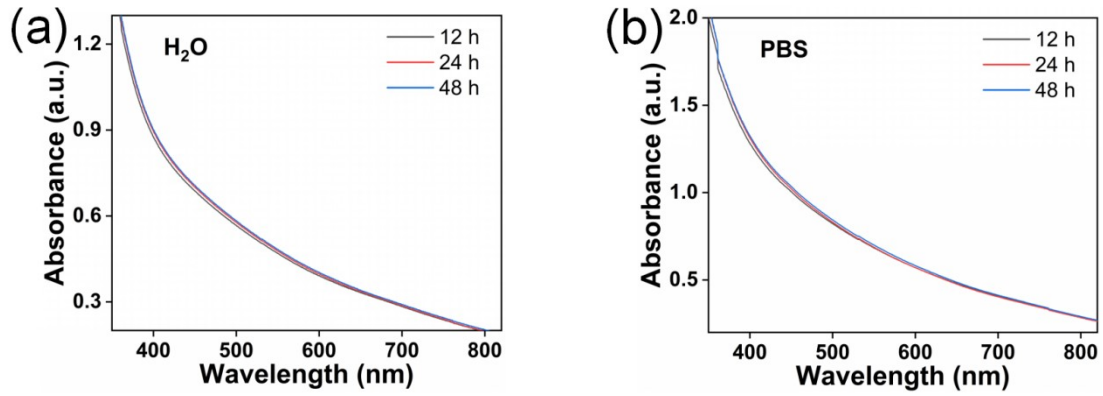

Fig. S1 The UV-vis absorbance spectrums of HMPDA-Cu@PAA NPs dispersed in H_2O and PBS at different time points (12, 24 and 48 h).

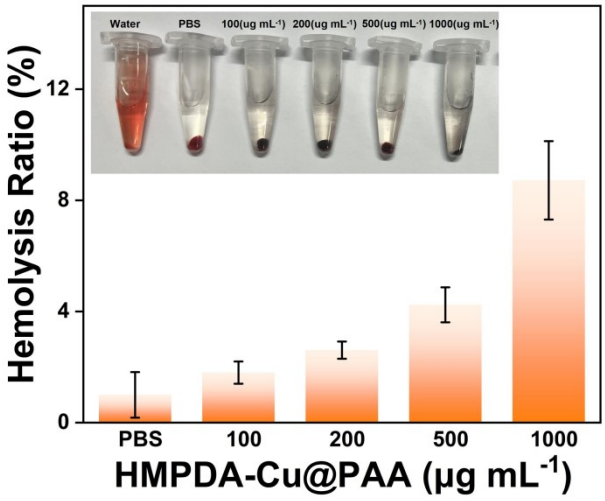

Fig.S2 Hemolysis assay of multiple densities of HMPDA-Cu@PAA NPs.

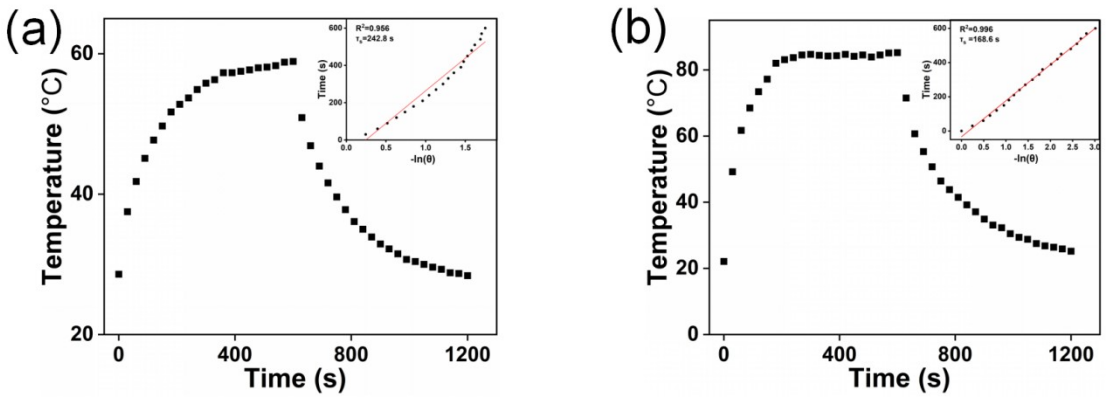

Fig. S3 Heating and cooling profiles of (a) HMPDA NPs, and HMPDA-Cu@PAA NPs along with inset displaying linear correlation between time and−ln θ data in the cooling phase.

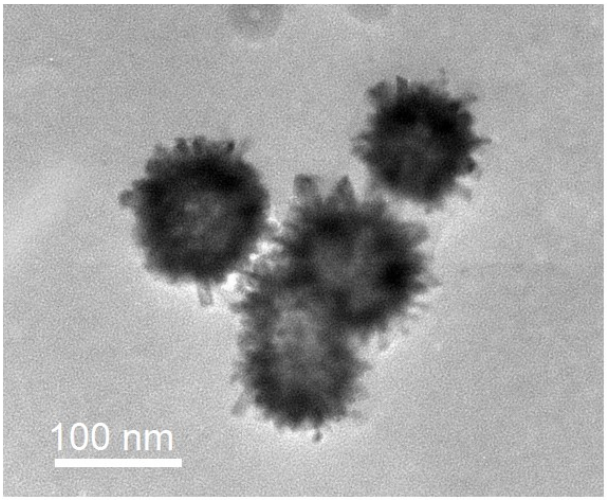

Fig. S4 TEM micrograph of HMPDA-Cu@PAA NPs after five irradiation cycles.

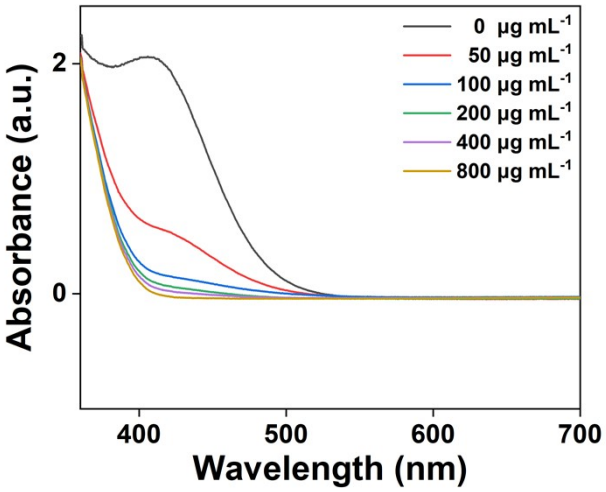

Fig. S5 The UV-vis absorbance spectrums of unreacted amounts of GSH after being mixed with different concentrations of HMPDA-Cu@PAA NPs.

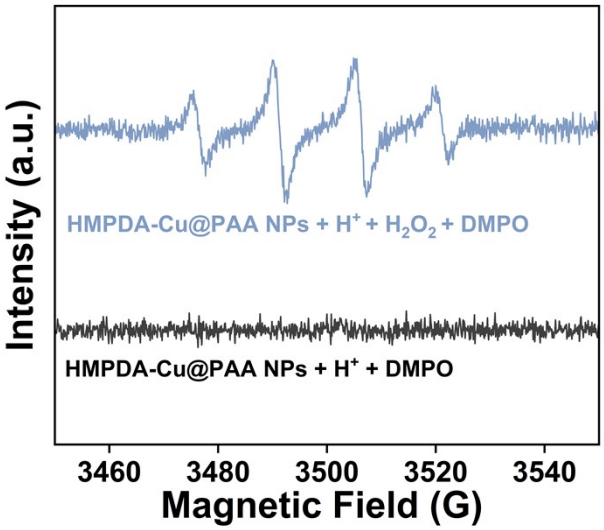

Fig.S6 EPR spectra of HMPDA-Cu@PAA NPs with different treatments.

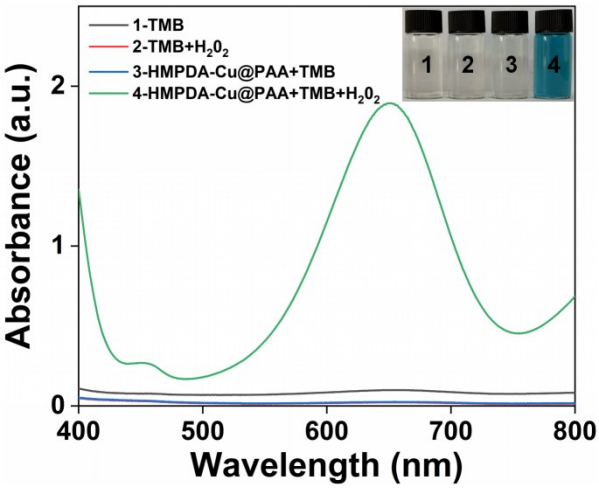

Fig.S7 Typical color change (inset) and corresponding UV-visible spectrum of HMPDA-Cu@PAA NPs catalytic oxidation of TMB by H_2O_2.

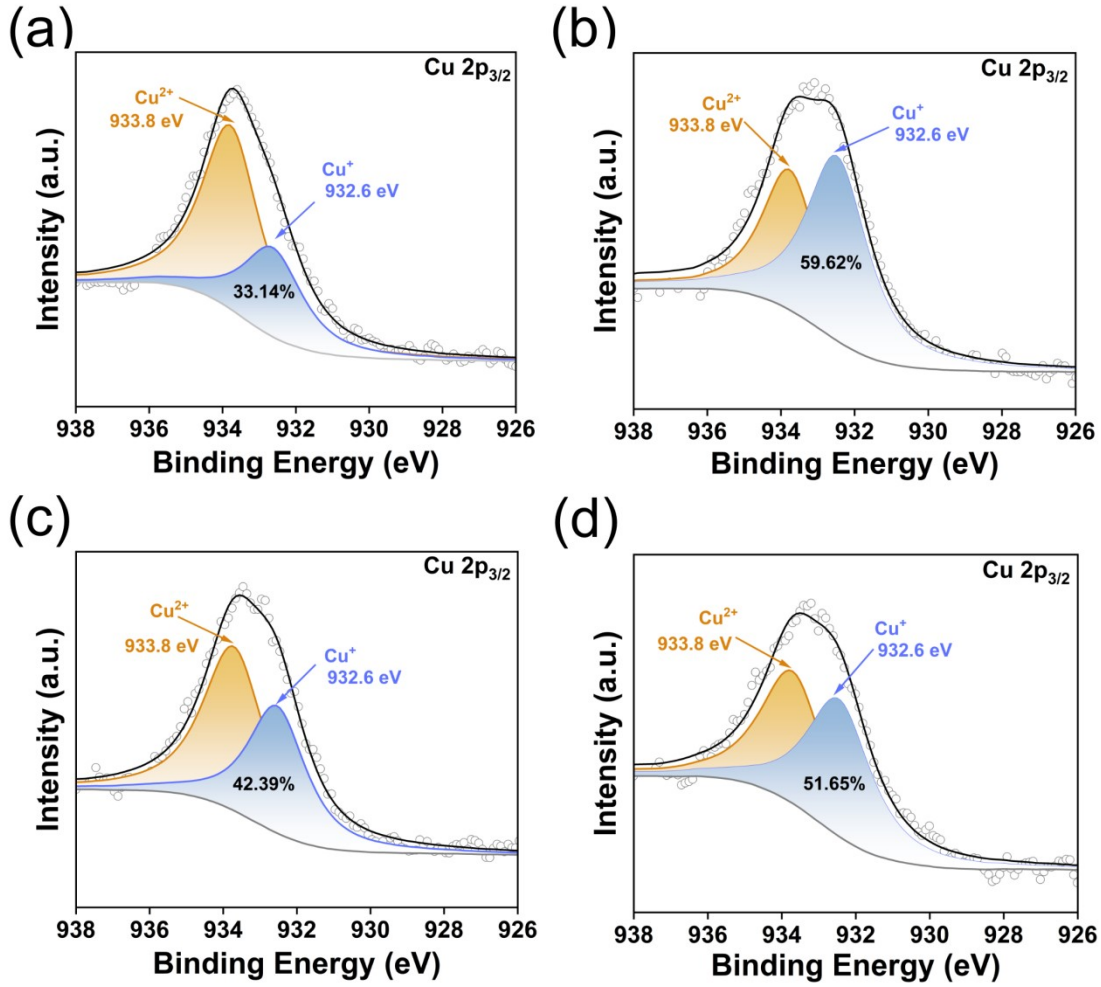

Fig. S8 High-resolution XPS spectra of Cu $2p_{3/2}$ for HMPDA-Cu@PAA NPs under different conditions: (a) HMPDA-Cu@PAA NPs before reaction, (b) after incubation with GSH (20 μM), (c) after treatment with H_2O_2 (100 μM), and (d) in the presence of both GSH (20 μM) and H_2O_2 (100 μM). The peaks at ~933.8 eV and ~932.6 eV are assigned to Cu^{2+} and Cu^{+}, respectively. The relative Cu^{+} content is labeled in each panel, indicating the variation of copper oxidation states under different reaction conditions.

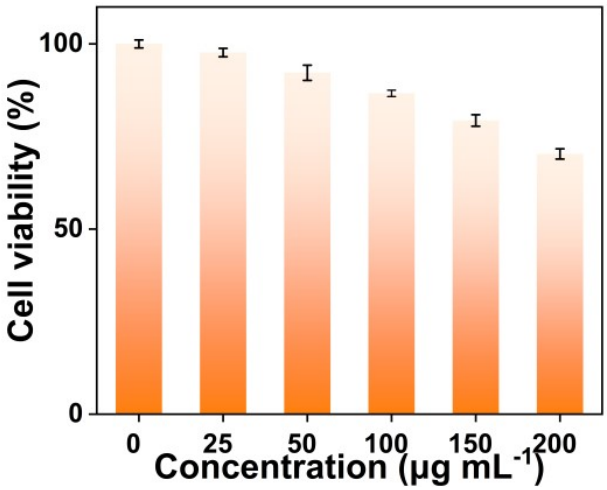

Fig.S9 Comparison of relative cell viability of L929 cells cultured with different concentration of HMPDA-Cu@PAA NPs for 24 h.

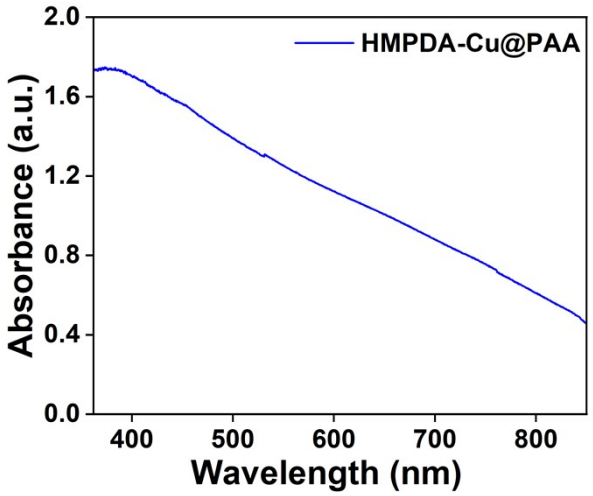

Fig. S10 The UV-vis absorbance spectrum of HMPDA-Cu@PAA NPs dispersed in DMEM medium containing 10% FBS and 1% streptomycin-penicillin.

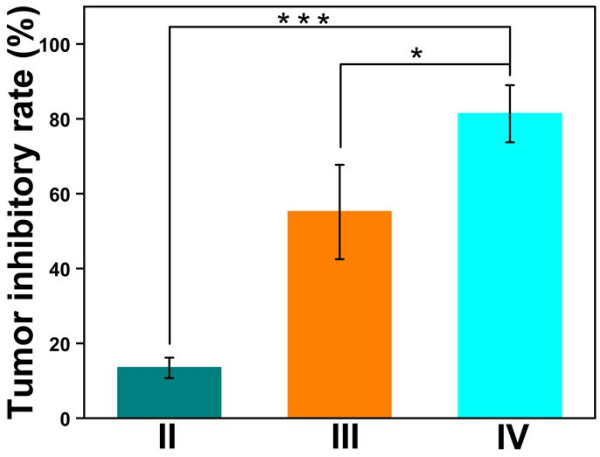

Fig. S11 The tumor inhibitory rate (TIR) of different groups. (n = 3) ***p < 0.001, **p < 0.01, *p < 0.05. The mice received treatment with the following groups: Group II by PBS plus 808 nm NIR laser, Group III by HMPDA-Cu@PAA NPs, Group IV by HMPDA-Cu@PAA NPs plus 808 nm NIR laser.

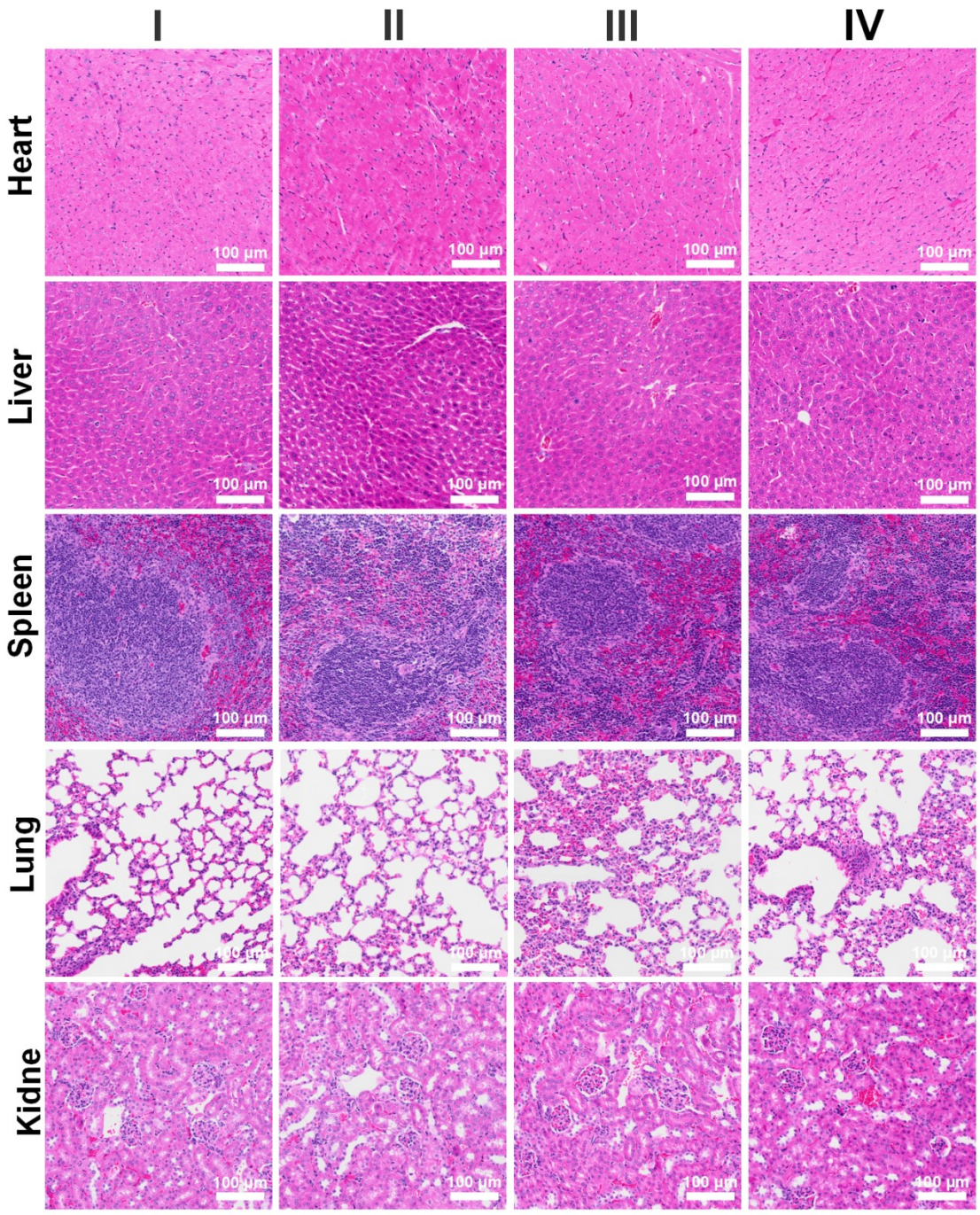

Fig. S12 Representative H&E staining images of major organs from MG63 tumor-bearing mice treated by PBS (I), PBS plus NIR (II), HMPDA-Cu@PAA NPs (III) and HMPDA-Cu@PAA NPs plus 808 nm NIR laser (IV), respectively. Scale bar: 100 μm

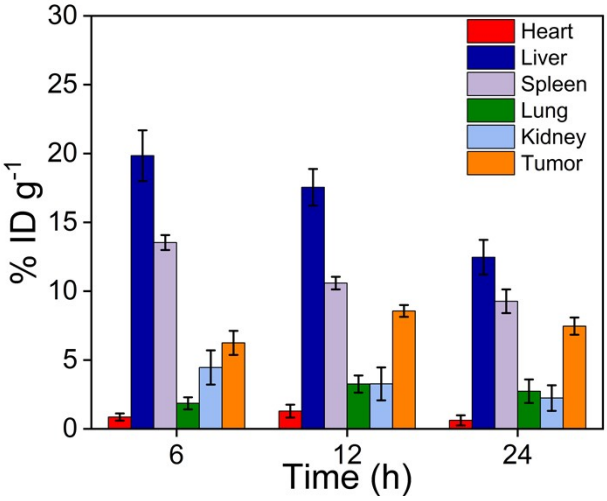

Fig.S13 Distribution of Cu element in major organs (heart, liver, spleen, lung, kidney) and tumors of mice at different time points after injection of HMPDA-Cu@PAA NPs.

3. Additional Tables

Table S1. Hematology analysis of healthy mice treated with PBS and HMPDA-Cu@PAA NPs.

Parameters	Units	Control	Treatment
WBC	$\times 10^9$/L	6.66 ± 2.63	4.36 ± 0.62
LYM	$\times 10^9$/L	5.26 ± 2.10	2.86 ± 0.59
MO	$\times 10^9$/L	0.77 ± 0.24	0.57 ± 0.21
GRA	$\times 10^9$/L	0.56 ± 0.24	0.89 ± 0.17
ESO	$\times 10^9$/L	0.06 ± 0.02	0.04 ± 0.01
BASO	$\times 10^9$/L	0.01 ± 0	0.01 ± 0
HGB	g/L	156.23 ± 24.43	186.51 ± 4.19
MCH	pg	16.41 ± 1.97	17.28 ± 0.24
MCHC	g/L	370.07 ± 43.93	396.50 ± 5.47
RBC	$\times 10^{12}$/L	9.68 ± 1.94	10.80 ± 0.39
MCV	fL	44.35 ± 1.31	43.58 ± 0.17
PLT	$\times 10^9$/L	770.19 ± 377.83	781.48 ± 178.07
PDW	fL	13.05 ± 1.00	12.95 ± 0.86

Table S2. Liver function tests of healthy mice treated with PBS and HMPDA-Cu@PAA NPs.

Parameters	Units	Control	Treatment
ALT	U/L	42.33 ± 3.86	39.67 ± 2.87
AST	U/L	214.67 ± 9.43	208 ± 4.97
AST/ALT	-	5.14 ± 0.73	5.26 ± 0.27
TP	g/L	73.33 ± 0.2	67.67 ± 1.70
ALB	g/L	38 ± 1.41	38.67 ± 2.05
GLOB	g/L	35.33 ± 2.87	29 ± 2.16
A/G	-	1.07 ± 0.05	1.37 ± 0.17
ALP	U/L	116 ± 17.45	135.33 ± 7.72
LDH	U/L	2849 ± 83.36	2860.33 ± 177.22

Reference

1. K. Lin, Y. Gan, P. Zhu, S. Li, C. Lin, S. Yu, S. Zhao, J. Shi, R. Li and J. Yuan, Nanotechnology, 2021, 32, 285602.
2. J. Yan, J. Zhang, Y. Wang, H. Liu, X. Sun, A. Li, P. Cui, L. Yu, X. Yan and Z. He, Adv Sci (Weinh), 2023, 10, e2207448.